Ceramic-Metal Interface Stability[1]

by

S. M. McDeavitt[1], G. W. Billings[2], and J. E. Indacochea[3]

Argonne National Laboratory
Chemical Technology Division
9700 S. Cass Ave.
Argonne, IL 60439

Phone: (630) 252-4308
Fax: (630) 252-9917
e-mail: mcdeavitt@cmt.anl.gov

To be Submitted to Proceedings from Joining of Advanced and Specialty Material
ASM International Materials Solutions 2001,
Indianapolis, IN
November 5–8, 2001

[1] Work supported by the U.S. Department of Energy, Nuclear Energy Research & Development Program, under Contract W-31-109-Eng-38

Ceramic-Metal Interface Stability

S. M. McDeavitt
Argonne National Laboratory, Argonne, Illinois
G. W. Billings
west CERAC , inc. (McCarran, NV)
J. E. Indacochea
University of Illinois at Chicago, Chicago, Illinois

Abstract

The goals in this investigation were to understand the interfacial chemical reactions between nitride ceramics and reactive liquid metals when exposed to elevated temperatures, and identify the microstructure changes regarding this region. Experiments were carried out where small metal samples of Zr were placed on top of selected nitride ceramic substrates (ZrN, HfN, and Hf_2N). The sample stage was heated in high-purity argon to about 2000°C, held for 15 minutes at the peak temperature, and then cooled to room temperature. An external video camera was used to monitor the in-situ wetting and interface reactions. Post-test examinations of the systems were conducted by scanning electron microscopy and energy dispersive spectroscopy. It was determined that the Zr is very active in the wetting of nitride ceramics at elevated temperatures. This interaction began at high temperatures before melting. A reactive transition phase formed between the ceramic and the metal. This layer was dense and continuous and it appears to be some form of zirconium nitride. A strong joint developed under these conditions also.

Introduction

Some of the most important physical and mechanical properties of new materials in modern applications are either controlled or are strongly affected by the presence and properties of interfaces. The metal-ceramic interfaces are essential in brazing of ceramics to metals, in producing ceramic metal composites, in electronic packaging systems, and in thin film technology. Often the bonding and adhesion between the ceramic and the metal is critical to the performance of a component. In addition, new materials with unique properties may be developed from multilayer ceramic-metal structures [1].

The study of metal-ceramic interfaces poses some formidable challenges both experimentally and theoretically. These extend from the difficulties of interface formation and structure, the nature and role of interdiffusion (and in general of the chemistry) at the interface, the nature and strength of bonding, the work of adhesion, to the complexity of understanding interface failure.

When bonding dissimilar materials, coating metal substrates with ceramics or fabricating composites, a transition layer needs to be formed to provide the link between the structurally different materials. Both chemical and physical factors play important roles in developing acceptable assemblies with adequate strength and overall properties [2]. In most cases one of the bonding phases is a liquid at the bonding temperature. Wetting and spreading are important phenomena in that they play a role in the localized chemical changes of the substrate surface and the liquid in contact with the substrate, in order to form

an intimate reaction layer without the application of pressure.

Wetting phenomena has been investigated extensively; early studies originated from the field of adhesion and waterproof treatment [3, 4]. The chemical reaction [5-7] or the mass transfer between the liquid and the solid had not been considered until the early 1970s. In those days, most metallurgists focused their investigation on soldering and brazing as an application of the wetting phenomena. However, wetting has also been important in the fields of casting, hot galvanizing, solidification, and in the fabrication of metal matrix composites using liquid metal. An important objective of our investigation has been the development of ceramic materials to be coated onto metal crucibles for melting reactive metals (Zr, Zr-stainless steel alloy and Uranium). The ultimate goal was to develop ceramic-coated crucibles that would not react nor be wetted by the reactive molten liquid. Titanium (as well as Zr and Hf) containing alloys even at low concentrations of Ti (Zr, Hf) ~2-5% show high degree of wettability with most solids – oxides, carbides, nitride ceramics and carbon substrates due to their very high chemical affinity for oxygen, carbon, nitrogen and other nonmetal elements [8].

The selection of the candidate ceramic materials was done by referring to the energy of formation of oxide, nitride or carbide ceramics. Thermodynamic calculations were carried out and plotted as function of temperature as an Ellingham-like diagram (Figure 1). The systems were chosen based on the largest negative magnitudes, since these represent the most stable structures. Therefore, according to equilibrium thermodynamics the oxides, which have energies of formation lower than that of the ZrO_2, e.g., BeO, CaO and Y_2O_3, are not expected to react with the molten Zr since in order for these oxides to be reduced, ZrO_2 should be formed and this is expected to be unlikely since the energy of formation of ZrO_2 is higher than those of BeO, CaO and Y_2O_3. Studies were undertaken on these systems and the results were discussed in earlier publications [9, 10].

These wetting behavior studies were carried out at temperatures up to ~2000°C and have unique application to ceramic joining issues. On the other hand, in the ceramic/metal joining field it is recognized that commercially available filler metals cannot be used at elevated temperatures, because commercially available filler materials for joining structural ceramics have low melting points. This in turn restricts the use of ceramics as part of a structure in very demanding service conditions.

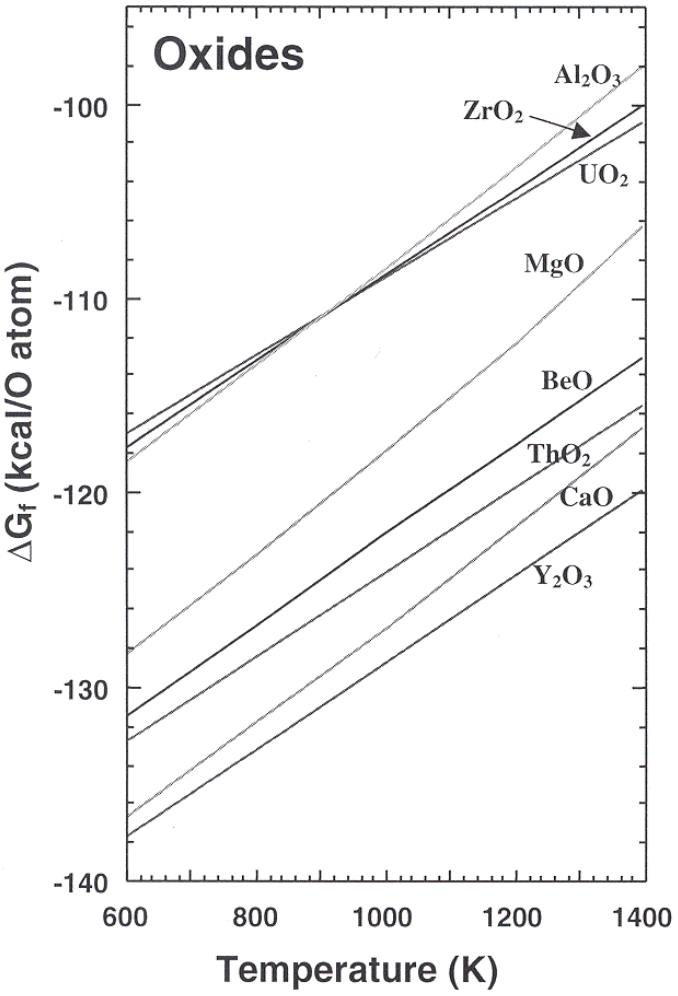

Figure 1. Standard free energy of formation of oxides as function of temperature. (Calculated).

Another aspect of this investigation is directed at developing filler metals that have a high melting point, but also do not dissolve or degrade the ceramic substrate. Zr has a high melting point and in view of its reactive properties, this investigation contemplates its use Zr in the development of high-temperature filler metals.

The work presented in this article considers the reactions at the ceramic-metal interface and the microstructures that develop during melting and exposures to the high temperatures. The results of the interactions between zirconium metal and the

zirconium and hafnium nitrides are examined and discussed.

Materials and Experimental Procedure

The substrate materials used in this portion of the investigation, ZrN and HfN, were processed using high purity powders with no sintering aids. The powders underwent a hot uniaxial pressing to about 90% density. The ceramic substrates once fabricated did not undergo any special surface finish. The melting of the metal samples and their exposure to the ceramic substrates were conducted by placing small metal specimens onto ceramic substrates. All materials were cleaned prior to the tests, using acetone to remove dirt and other contaminants from the materials. The two metal specimens utilized were pure Zr and Zr + 8 wt. % ferritic stainless steel. The composition of the stainless steel (HT-9) in weight percent is 0.5Ni, 12.0Cr, 0.2Mn, 1.0Mo, 0.25Si, 0.5W, 0.5V, 0.2C, and balance Fe. The metal/ceramic combination was heated in a tungsten mesh furnace in high purity argon cover gas with a sensing thermocouple placed about 0.5 cm beneath the samples. The materials were preheated to 600°C, continuously heated at a rate of about 50°C/min to 1500°C, 20ºC/min to 1800ºC and then at 10°C/min to 2212°C. The samples were held at 2212ºC for 15 minutes, and then cooled at uncontrolled rate by shutting down the furnace. In most cases, the peak temperature was held for 5 min and then cooled at ~20°C/min.

The wetting and high temperature interactions between the molten metals and ceramic substrates were monitored through an external video camera. A schematic of the high temperature furnace and setup is shown in Figure 1. In-situ observations were followed by post-test examinations using scanning electron microscopy (SEM) and energy dispersive spectroscopy (EDS).

Results and Discussion

Zr metal / ZrN Interactions

Results of the interaction between Zr metal and ZrN were presented in an earlier publication [9, 10].

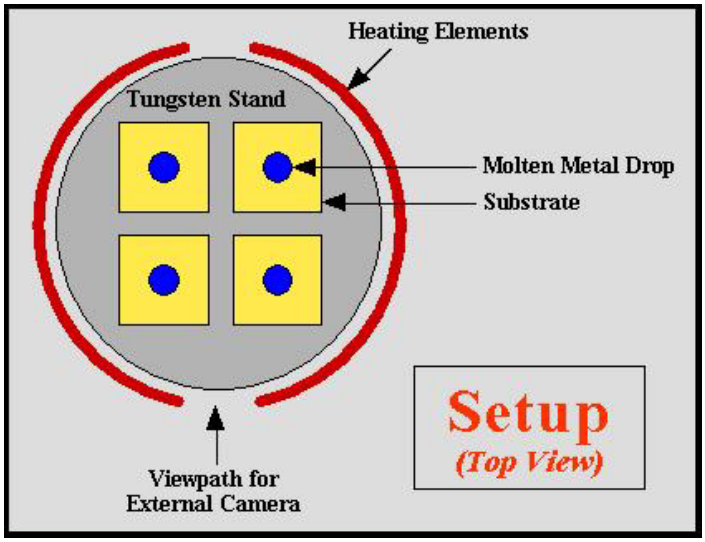

Figure 2. Schematic of the furnace and setup of the high temperature experiments.

Zr did not melt at its established melting point of 1855ºC, but instead the Zr specimen began melting at 1975ºC, and it was completely molten at about 2000ºC. A posttest examination of the system showed a strong bonding between the Zr metal and the ZrN. A new dense reaction layer developed between the solidified metal and the ceramic substrate. The region in the substrate immediately adjacent to the reaction layer showed a discoloration band, evidence of a chemical reaction about the interface between the pure Zr and the ZrN. The microstructure of the Zr metal has the characteristics of a solidified alloy, which indicates that nitrogen from the dissociation of the original ZrN substrate, must have diffused into the liquid Zr and dissolved there. A new $ZrN_{(1-x)}$ phase formed. This newly formed $ZrN_{(1-x)}$ was found to be present as laths throughout the Zr metal, and as a uniform band, about 35 to 45 μm thick, intimately bonded to the original ZrN substrate. This band appears much denser than the substrate, and it also shows a long crack that extends the length of the metal/ceramic interface. There was observed some crack branching form the main crack, but all the cracking was limited to the this band. The cracking is caused by the difference in the thermal expansion coefficients. Figure 3, a SEM micrograph shows, the changes in the microstructure of the pure Zr metal and the formation of the $ZrN_{(1-x)}$ all through this system.

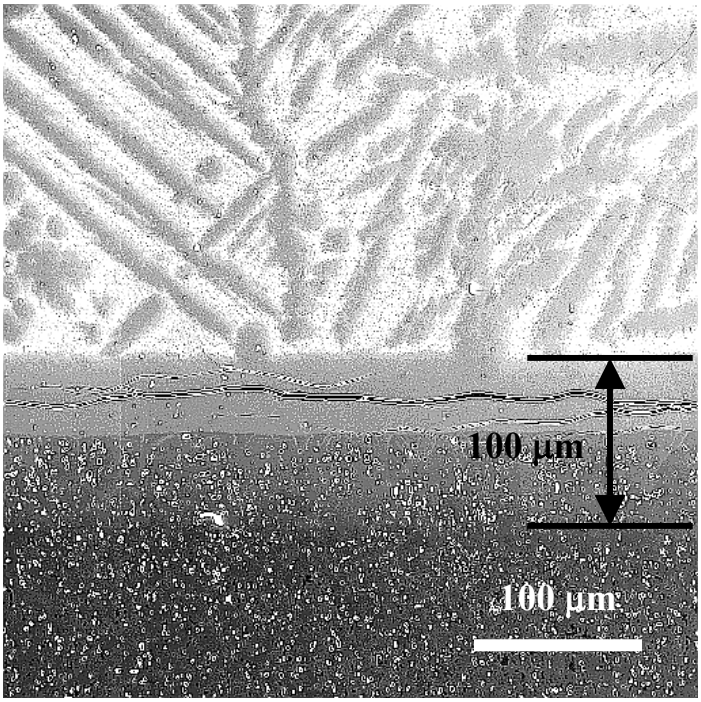

Figure 3. SEM micrograph of the Zr-ZrN showing changes in the microstructure of the Zr metal and reactions at the metal/ceramic interface.

By referring to the partial equilibrium phase diagram [11] in Figure 4, and considering that melting did not occur until about 1975°C, it is reasonable to estimate that the amount of nitrogen dissolved in α-Zr, would exceed 20 atomic percent.

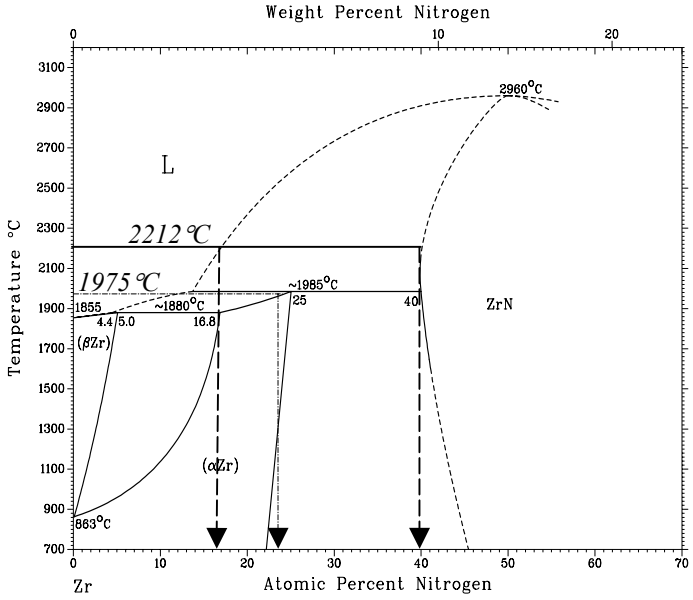

Figure 4. Partial equilibrium phase diagram of zirconium and nitrogen [11].

Between 1975 and 1985°C, the equilibrium phases are α-Zr, at a composition of ~20 at. % N and a small amount of liquid, at a composition of ~12 at. % N. Then as the system was heated above the peritectic temperature (~1985°C) and held at the peak temperature of 2212°C, the resulting equilibrium phases are liquid and ZrN. Some of the α-Zr melts and mixes with the liquid already present before the peritectic temperature, reaching an equilibrium composition of ~17 at. % N; the remaining α-Zr dissolves more nitrogen and transforms to to a new *ZrN* with an equilibrium composition of ~ 40 at. % N. Since the source of the nitrogen is the ZrN substrate, it is reasonable to assume that the bulk of the new $ZrN_{(1-x)}$ will form at the interface with the ceramic substrate as shown in Figure 3. The solidified metal structure is dendritic. From the microstructure of the solidified metal, it is estimated that the amount of the second phase (ZrN) is approximately 40-50%, which accordingly to the phase diagram the composition of the new Zr-N alloy can be approximated to be 30 at. % N. As the temperature drops, the liquid undergoes a peritectic reaction; the new alloy is hypoperitectic.

It is noted that the ZrN substrate did not undergo major degradation. Furthermore, the interfaces, between the ZrN-substrate and the newly formed $ZrN_{(1-x)}$, and the interface between the $ZrN_{(1-x)}$ and the solidified metal alloy are both smooth, which suggests that the solubility of the reaction products in the molten Zr, provides the mechanism for the immediate removal of the reaction products. It is also observed at the interface some discoloration of the substrate about 50-60 μm; this change most likely reflects a change in the composition of the ZrN, rather than an stoichiometric change in light of the wide composition phase of this phase field as shown in the phase diagram. It is also likely that the newly formed $ZrN_{(1-x)}$ has the same stoichiometry as the ZrN as dictated by the equilibrium phase diagram. The difference in the appearance of the newly formed $ZrN_{(1-x)}$ compared to the ZrN-substrate is more the result of method of formation. That is, sintered versus precipitation from the supersaturated Zr liquid metal.

The chemical reaction between the Zr metal and the ZrN was expected in view of the magnitudes of the energies of formation of the nitrides compared to

those of stable oxides, as shown in Figures 1 and 5. Hence, it would be expected of nitrides to reduce sooner than oxides if exposed to Zr metal under similar conditions of temperature and type of atmosphere.

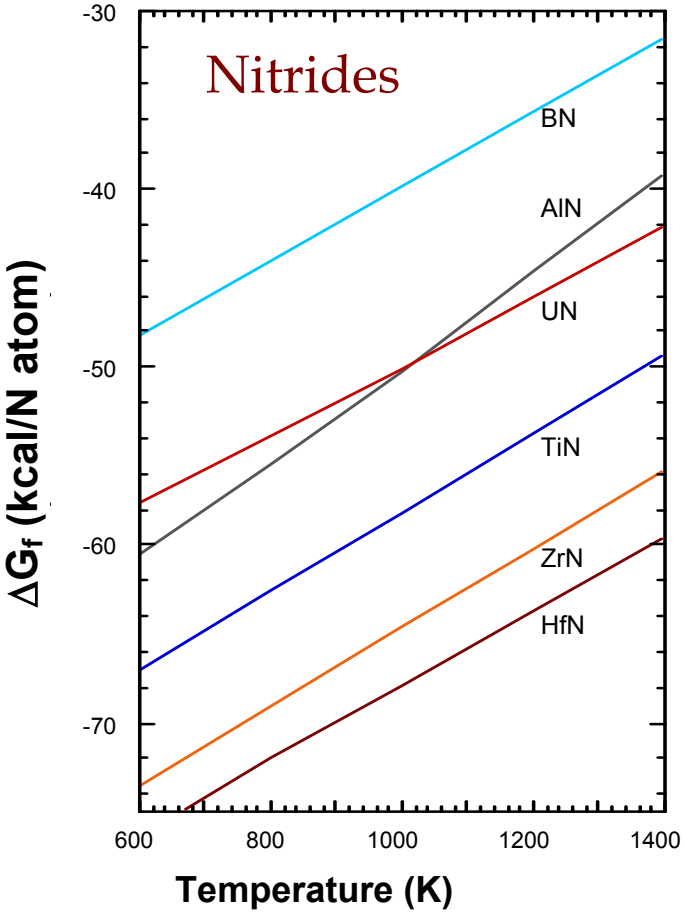

Figure 5. Standard free energy of formation of nitrides versus temperature. (Calculated).

Zr metal / HfN Interactions

Melting of the Zr metal was delayed until about 2000°C, and melting was complete at ~2100°C. But the whole system, as in the previous case, was heated to a peak temperature of 2212°C and held for 15 minutes. The suppression of the melting behavior suggests nitrogen contamination of the Zr metal, and definitely the HfN substrate is the source. The transfer of nitrogen begins below the melting point of Zr. The general chemical reaction can be written as follows:

$$\mathbf{HfN_{(s)} + Zr_{(s)} \rightarrow HfN_{(1-x')} + a\ ZrN_{(1-x'')} + b\ Zr(\alpha)_N + c\ N_2}$$

Post melting observations with the naked eye of the specimen showed the Zr metal bead had a golden color, given qualitative evidence of the nitriding of the Zr.

The metallographic analysis of the Zr/HfN system was done using the scanning electron microscope. Figure 6 illustrates the changes that occur in the Zr metal and at the metal/ceramic interface during the heating and cooling cycle. It is observed that the microstructure of the Zr metal in this system is very similar to the microstructure in the Zr/ZrN system just discussed, shown in Figure 3. As mentioned at the beginning of this section, the nitrogen coming from the reduction of the HfN, is what alloys the Zr-metal. The similarity in microstructure and the fact that the new Zr-N alloy does not melt until ~2000ºC, it suggests a composition very similar to the previous system. It can be seen that the $ZrN_{(1-x)}$ precipitated as laths through out the α-Zr matrix and at the interface with the HfN substrate.

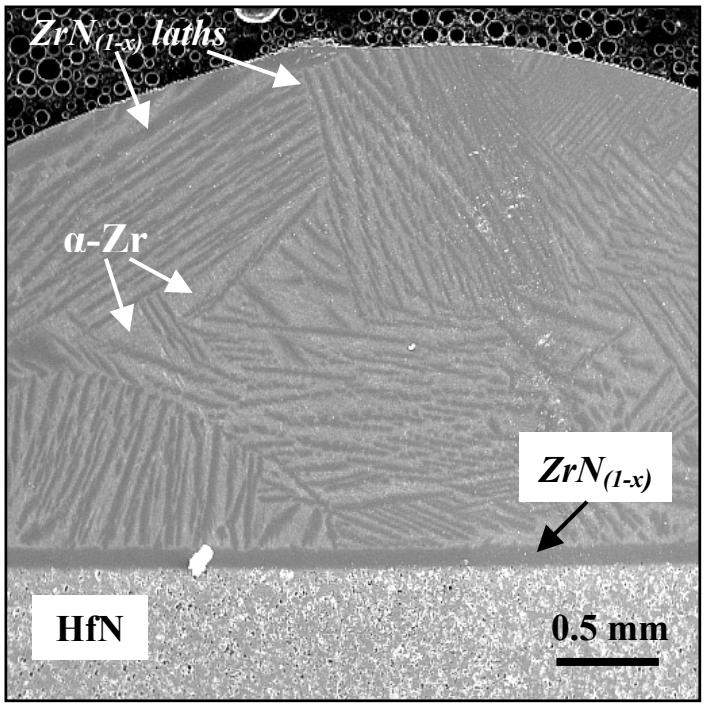

Figure 6. SEM micrograph of the Zr metal bead interaction with the HfN during heating and cooling.

As described in the previous section the alloyed molten Zr when it reaches 2212ºC, its equilibrium structure will consist of liquid and $ZrN_{(1-x)}$with compositions defined by the equilibrium phase diagram in Figure 4. Estimates of the phase volume fractions of the α-Zr and $ZrN_{(1-x)}$ are alike the case before, which further confirms that both alloys are the same. That is, this alloy is hypoperitectic.

For an understanding of the reactions occurring in the HfN, we can refer to the Hf-N equilibrium phase diagram [11] shown in Figure 7. The HfN substrate corresponds to a composition of 50:50 Hf to N at. %.

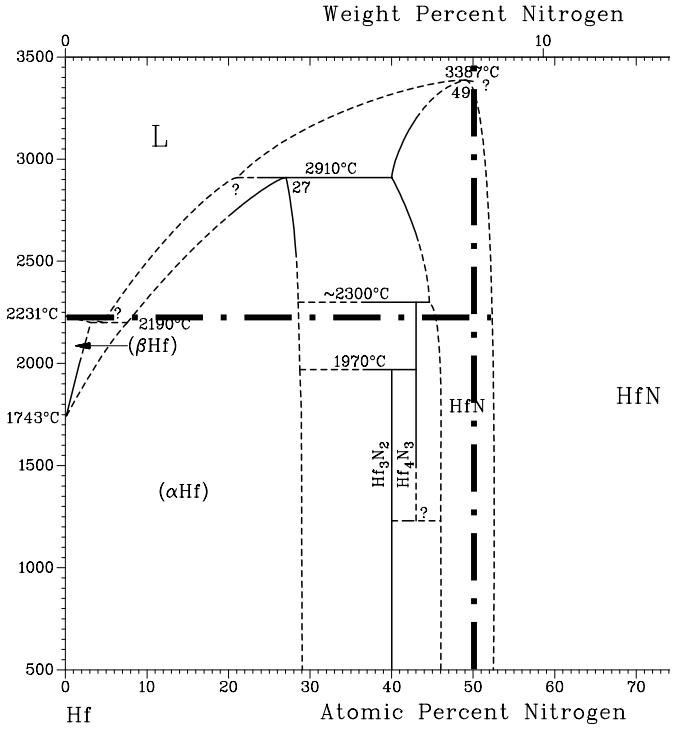

Figure 7. Partial equilibrium phase diagram of hafnium and nitrogen [11].

As the Zr metal is heated in contact with the HfN, according to low temperature thermodynamics, the substrate should not react with the Zr and form ZrN, since HfN is more stable (Figure 5). However, as we have seen in other systems in our investigation [9, 10] the stability of ceramics in contact with liquid metals at elevated temperatures cannot be explained using lower temperature data. If we look at partial phase diagram for Hf and N at 2212ºC, (Figure 7), the HfN phase has a composition range of 46 to 53 at. % nitrogen, which suggest that for a small reduction in the amount of nitrogen in HfN, the stoichiometry of this phase would not change. The extent of the microstructural changes (discoloration) in the HfN near the interface was not significant, as seen in Figure 8. This implies that in view of the mass of the Zr metal the amount of nitrogen needed to saturate the liquid and equilibrate the system at 2212ºC was so small that might not have changed the stoichiometry of the substrate even at a location adjacent to the $ZrN_{(1-x)}$.

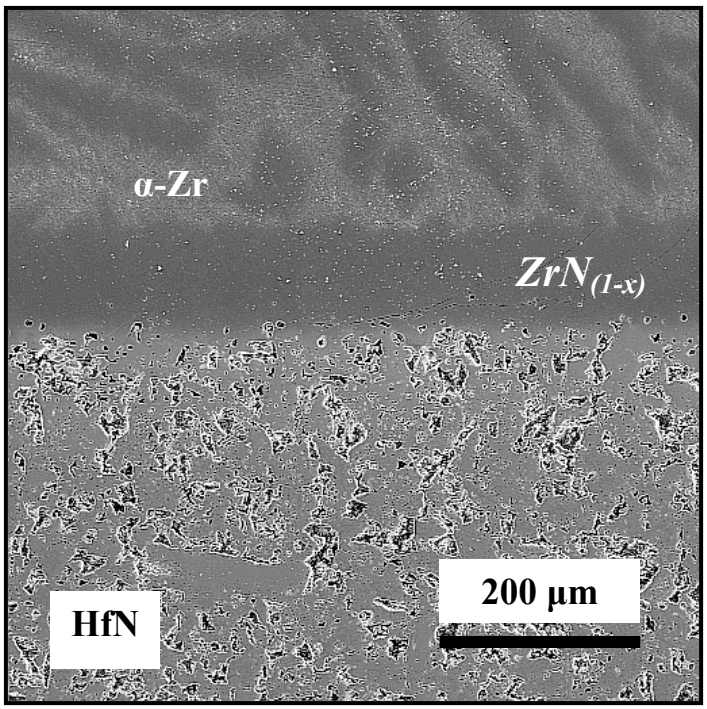

Figure 8. SEM micrograph illustrating the condition of the interface in the Zr/HfN system.

The $ZrN_{(1-x)}$ that formed at the interface with the HfN is fairly uniform in thickness and appears very dense compared to the HfN substrate, analogous to what it was found in the Zr/ZrN system (Figure 3). No major cracks were observed at this reaction layer. The region in the substrate adjacent to the reaction layer does not show microstructural evidence of α-Hf being formed (e.g., discoloration), even when seen at large magnifications (Figure 9). Furthermore, the phase diagram shows that at the holding temperature of 2212ºC the HfN must have a reduction of ~5 at. % N in HfN to have Hf_4N_3 and ~7 at. % N to see α-Hf.

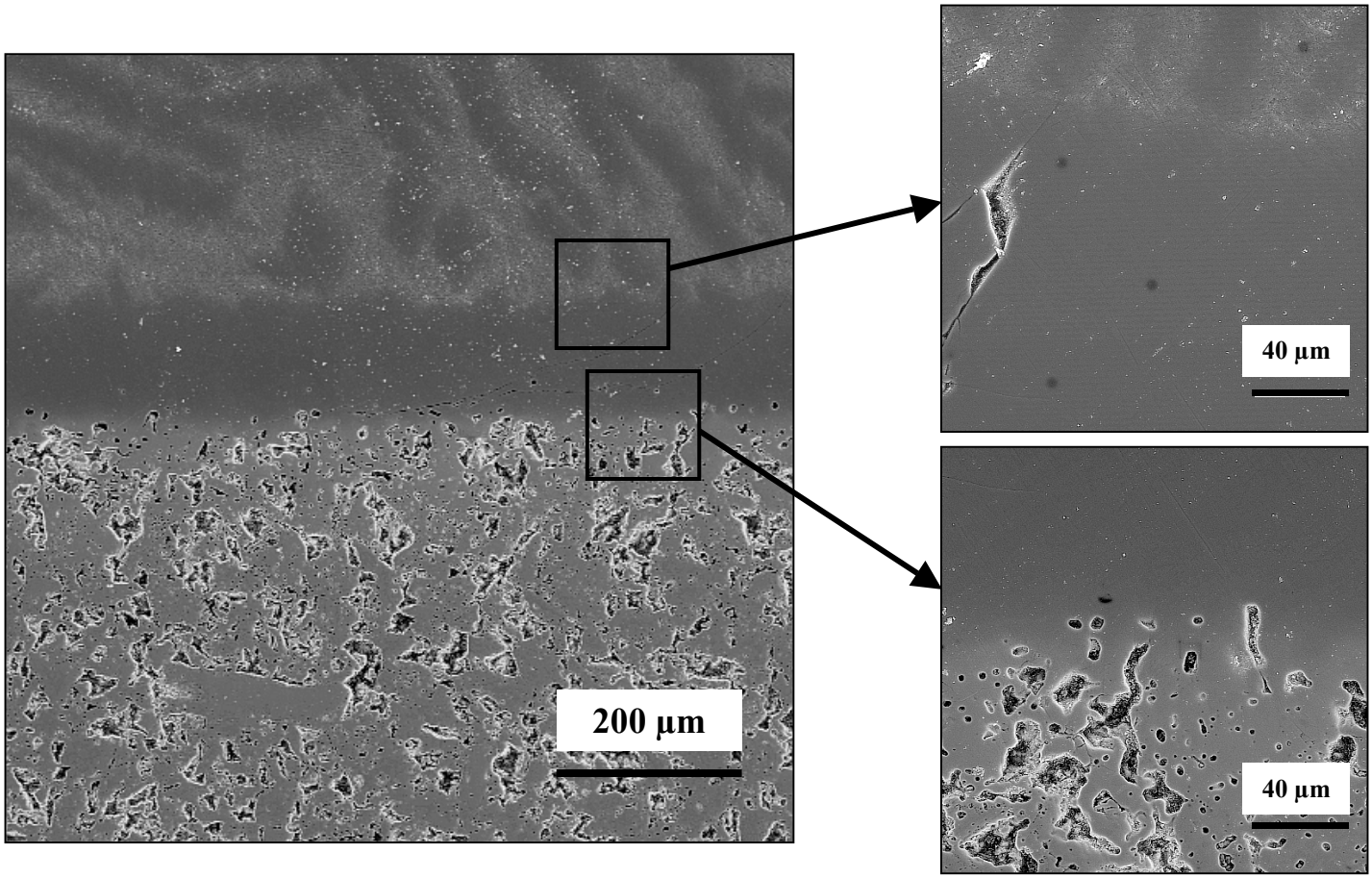

Figure 9. SEM micrograph of the interface of the Zr metal – HfN substrate, after the heating and cooling cycles. The system was held at 2212ºC for 15 minutes. The atmosphere was ultra high purity argon.

Because of the limitations of our EDX detector with respect to the light elements, such as nitrogen, it was not possible to resolve any of the HfN stoichiometries or the presence of α-Hf. Yet the micrographs shown in Figure 9 do not indicate the presence of any other phase besides the HfN. It shows a continuous HfN phase all the way to the reaction layer.

The composition of the reaction layer and of the adjacent regions by EDX in terms of the presence of zirconium and hafnium was determined at selected spots as shown in Figures 10 and 11. This analysis was mostly qualitative. It was observed that those spots located at the upper half of the reaction layer, and those in the solidified Zr-alloy, showed only Zr peaks (Figure 10). In the lower portion of the 150-µm thick reaction layer, a transition from Zr to Hf rich regions was observed, yet the Zr peak was found to be more prominent than the Hf peak throughout the reaction layer even at the spots near the lower portion of this reaction layer. Figure 11, top EDX spot, for example, shows a dot about 30 µm from the interface of the HfN substrate with the reaction layer, where the Zr peak proves more prominent than the Hf peak. The EDX spot analyses done at the lower portions of the layer showed Hf peaks, but the Zr peak still appears prominent. The intensity of the Hf peaks were higher only when the analysis was performed in the HfN next to the reaction layer. Even at this site Zr was detected. The absence of Hf from most of the reaction layer and from the Zr-N alloy is partly due to the limited reduction of HfN. In other words, because of the size of the Zr metal one can speculate that only a small amount of nitrogen was needed to saturate the α-Zr and the liquid-Zr at 2212ºC, and it is likely that the amount of nitrogen loss by the HfN is not large enough to generate different stoichiometric HfN's.

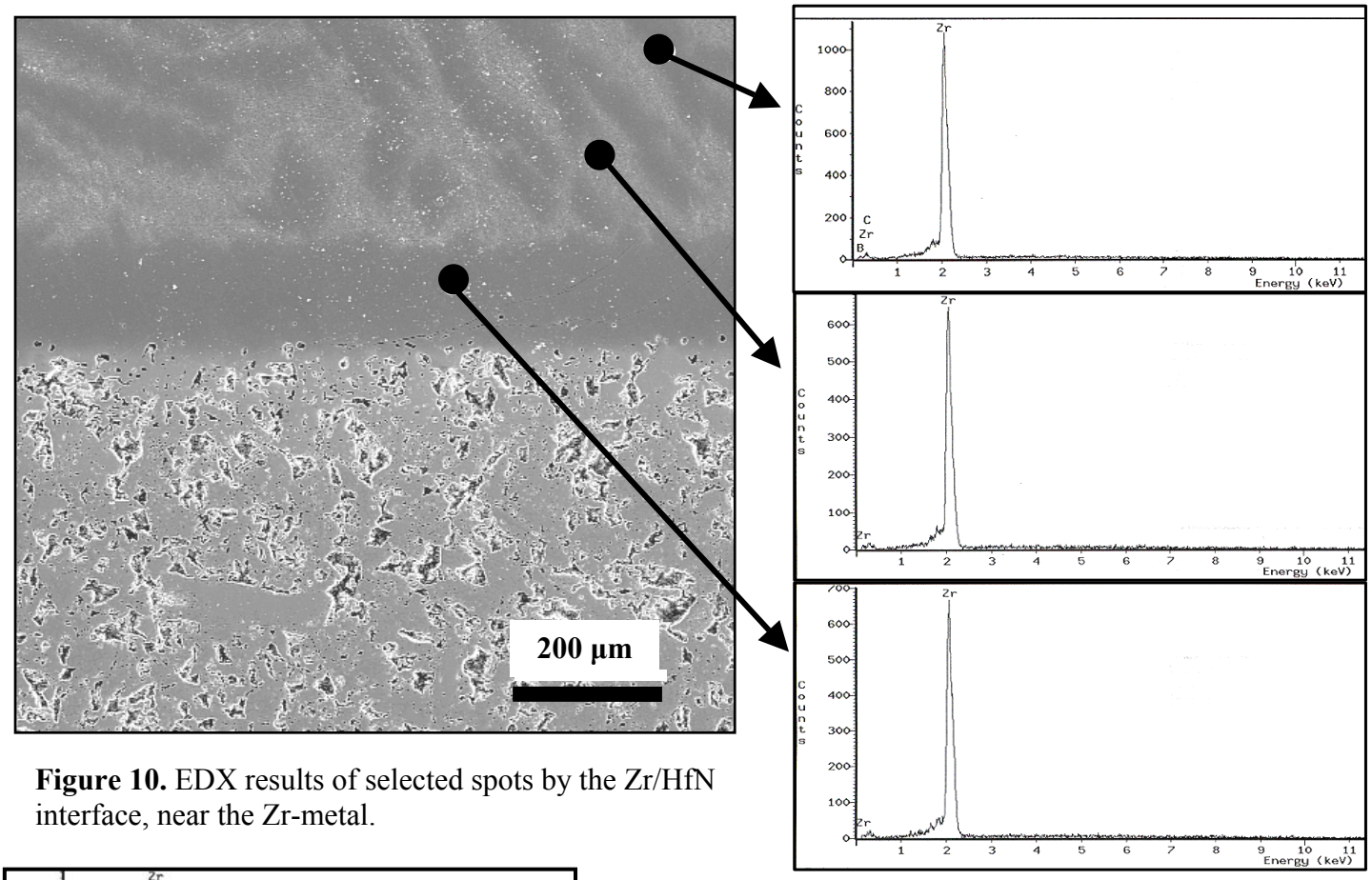

Figure 10. EDX results of selected spots by the Zr/HfN interface, near the Zr-metal.

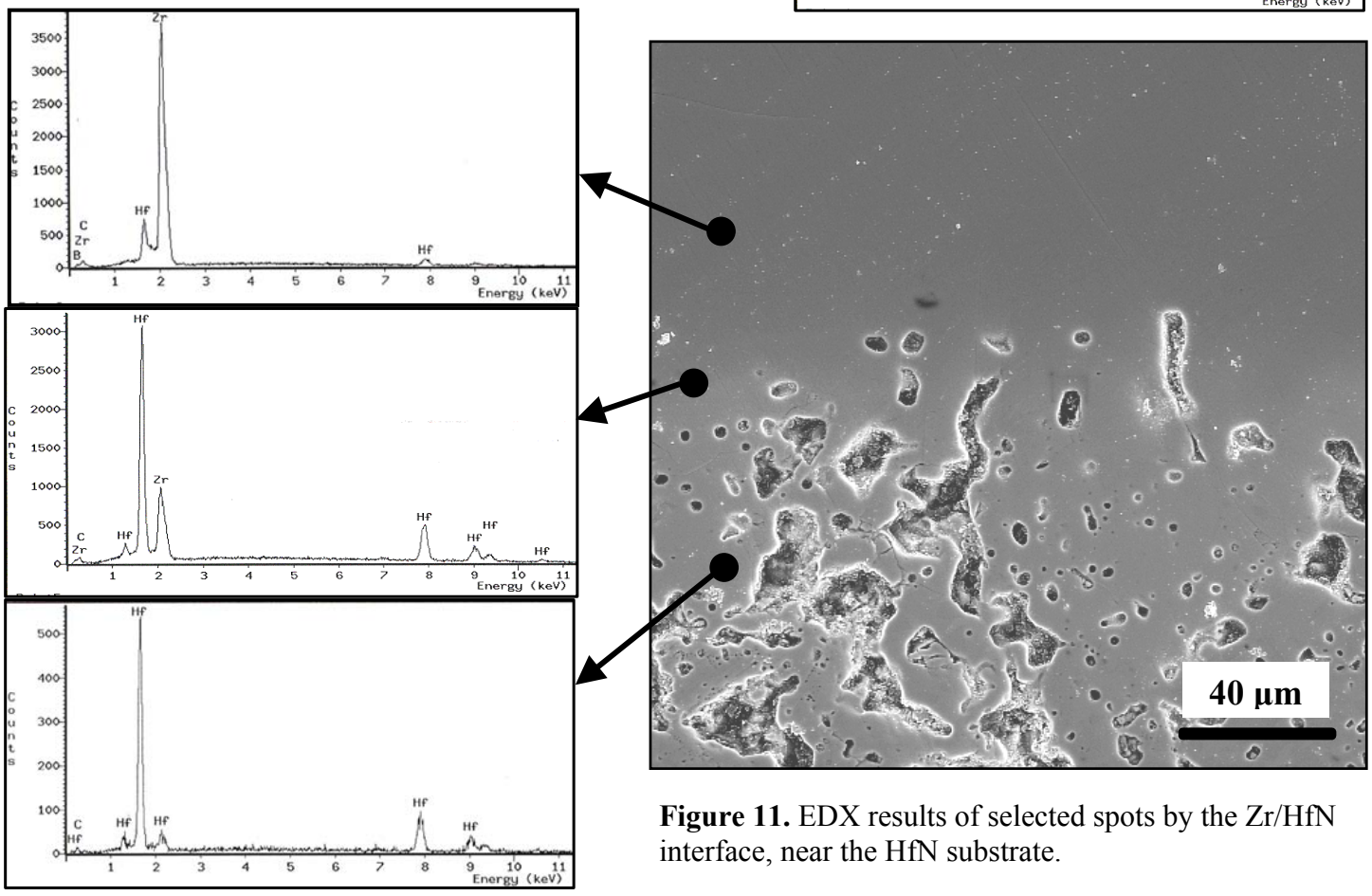

Figure 11. EDX results of selected spots by the Zr/HfN interface, near the HfN substrate.

Zr metal/ Hf_2N Interactions

When Zr metal melted in Hf_2N, it reacted similarly to the case of Zr/HfN. That is, a reaction layer formed at the metal side of the Zr/ ceramic interface. The reaction layer is $ZrN_{(1-x)}$, which is denser than Hf_2N substrate, was observed to be also very uniform in thickness. It did not contain major cracks, as it was the case with the Zr/ZrN system, but it had minor cracking, which was greater than that found in the Zr/HfN system. The microstructure of the resolidified Zr, is also identical to that of the Zr/HfN, i.e., an α-Zr matrix with $ZrN_{(1-x)}$ imbedded in it. These microstructural characteristics can be observed in Figure 12. The solidified metal bead was found to have wetted the ceramic substrate and it bonded strongly to it. Some cracking was found in the ceramic substrate adjacent to the reaction layer, particularly at those locations where the spreading of the molten alloy ended.

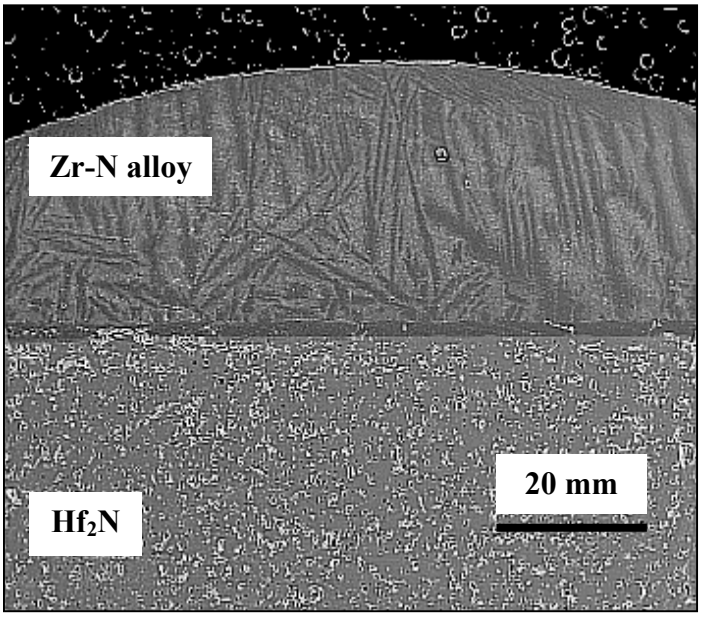

Figure 12. SEM micrograph of the Zr-metal bead interaction with the Hf_2N during heating and cooling.

EDX analysis of the solidified metal bead and of the reaction layer reveals that only Zr is present at these locations. Hf was found to be present only in the lower portion of the reaction layer near the Hf_2N substrate. Similarly, Zr did not diffuse into the ceramic substrate, some small peaks of Zr were detected at the lower regions of the reaction layer and in the ceramic substrate immediately next to this layer. No microstructural changes could be resolved in the ceramic substrate near the interface. These results were identical to what it was observed in the Zr/HfN system.

Conclusions

1. Zr was found to undergo intensive interactions with ZrN, HfN, and Hf_2N.
2. The interaction between Zr and the nitride substrates starts off before any melting takes place. Nitrogen diffuses from the nitride substrates and dissolves in the solid Zr-metal.
3. The higher melting point of the Zr metal and the golden color of the metal bead are evidence of the diffusion of nitrogen and its dissolution in the Zr bead.
4. The reaction layer found between the Zr-bead and the ZrN, HfN and Hf_2N is rich in Zr and most likely some type of nitride stoichiometry of zirconium, $ZrN_{(1-x)}$. This layer was found to be much denser than the ceramic substrates.

References

1. L. Magaud and A. Pasturel, Proceedings of the Second International Conference on High Temperature Capillarity, HTC-97, p. 3. Krakow, Poland (1997).
2. J.A. Pask and A.P. Tomsia, Engineered Materials Handbook, Vol. 4, pp. 482-492, ASM International (1991).
3. Contact Angle, Wettability, and Adhesion: Advances in Chemistry Series 43, American Chemical Soc., 1964.
4. Contact Angle, Wettability and Adhesion: K.L. Mittal Ed., VSP, Utrecht, 1993.
5. I.A. Aksay, C.E. Hogan and J.A. Pask: Surfaces and Interfaces of Glass and Ceramics, Materials Science Research. Vol.7, (1973) 299.

6. H. Nakae, H. Fujii, and K. Sato: Mater. Trans. JIM, 33(1992) 400.
7. L. Espi, B. Drevert, and N. Eustathopoulos: Metall. and Mater. Trans., 25A(1994) 599.
8. Y.V. Naidich and V.P. Krasovsky. Proceedings of the Second International Conference on High Temperature Capillarity, HTC-97, p. 87. Krakow, Poland (1997).
9. S.M. McDeavitt, G.W. Billings and J.E. Indacochea, Proceedings of the Internati Symposium on Joining of Advanced and Specialty Materials IV, p. 36-42. St. Louis, MO (2001).
10. S.M. McDeavitt, G.W. Billings, and J.E. Indacochea, "Fundamental studies of ceramic-metal interfacial reactions at elevated temperatures", Brazing, High Temperature Brazing and Diffusion Welding, DVS Proceedings, Vol. 212, pp 189-194, 2001.
11. Binary Alloy Phase Diagrams, Second Edition, ASM International (1990).